Arabian Journal of Geosciences (2021) 14: 766
https://doi.org/10.1007/s12517-021-07030-5

ORIGINAL PAPER

Late Quaternary paleoclimatic and paleoenvironmental changes in the Konya Closed Basin (Konya, Turkey) recorded by geochemical proxies from lacustrine sediments

Hükmü Orhan[1] · Arif Delikan[1] · Ahmet Demir[2] · Sevinç Kapan[3] · Kemal Olgun[4] · Ayhan Özmen[5,6] · Ülkü Sayın[5,6] · Gamze Ekici[5] · Hülya Aydın[7] · Birol Engin[7] · Recep Tapramaz[8]

Received: 22 January 2020 / Accepted: 29 March 2021 / Published online: 22 April 2021

Abstract

The Konya Closed Basin is an important basin in central Turkey, in terms of its geographic position, Quaternary infills, and well-preserved archeological sites. It comprises Quaternary lake marls and other, mainly fine grained, sediments with locally in excess of 400 m. Geochemical data for samples taken from the 7-m-deep Adakale trench from the late Quaternary lacustrine sediments in the Konya Closed Basin are presented and have been used as proxies to elucidate the past climatic changes, weathering regime, redox conditions, and productivity. Climate changes observed in the studied samples for last 50,000 years were represented by oscillations in weathering processes, detrital input, redox conditions, water levels, and paleoproductivity. Geochemical data show that three periods of high detrital input (high Si+Al+K+Ti+Fe, high Ti/Al, Rb/Sr, low Ca and low Si/Ti), four periods of anoxic conditions (low Mn and Th/U and high Ni/Co, Mo/Al and V/Cr), and four periods of higher productivity (high Cu/Al, Ni/Al, Ca/Al, Ba/Al Si/Ti and Ca/Ti) were effective in the study area. These periods are corresponding to climatic changes during last glacial periods, the warm climate of Dansgaard-Oeschger (D/O) events (D/O 2-12) and the cold climate of Heinrich events (H 2-5).

Keywords Konya Closed Basin · Quaternary · Paleoclimate · Geochemical proxy · ESR dating

Responsible Editor: Attila Ciner

✉ Hükmü Orhan
horhan@ktun.edu.tr

Arif Delikan
adeli@ktun.edu.tr

Ahmet Demir
ahmetdemir136@gmail.com

Sevinç Kapan
sevinckapan_yesilyurt@hotmail.com

Kemal Olgun
kemalolgun@dsi.gov.tr

Ayhan Özmen
aozmen@selcuk.edu.tr

Ülkü Sayın
ulkusayin@gmail.com

Gamze Ekici
gamzebakkal88@gmail.com

Hülya Aydın
aydin.hulya8@gmail.com

Birol Engin
birol.engin@deu.edu.tr

Recep Tapramaz
recept@omu.edu.tr

[1] Department. of Geological Engineering, Konya Technical University, Konya, Turkey

[2] Department of Geological Engineering, Selçuk University, Konya, Turkey

[3] Department.of Geological Engineering, Çanakkale 18 Mart University, Çanakkale, Turkey

[4] DSİ 4. Regional Directory, Konya, Turkey

[5] Department of Physics, Selçuk University, Konya, Turkey

[6] Selçuk University Advanced Technology Research & Application Center, Konya, Turkey

[7] Department of Physics, Dokuz Eylül University, İzmir, Turkey

[8] Department of Physics, Ondokuz Mayıs University, Samsun, Turkey

Introduction

Lacustrine sedimentation is controlled by numerous interacting factors such as climate, tectonic, geomorphology, surrounding vegetation, aquatic biota, and recently human activities (Cohen 2003; Martín-Puertas et al. 2011; Guimaraes et al. 2016; Zhao et al. 2016). Lakes may respond rapidly to changes in these factors. Sediments deposited at the bottom of lakes have high potential to preserve the signs of these changes. Geochemical data obtained from lake sediments have been used to elucidate the past climatic changes, weathering regimes, redox conditions, regional vegetation covers, and human activities (Koinig et al. 2003; Eusterhues et al. 2005; Selig et al. 2007; Tanaka et al. 2007; Moreno et al. 2008; Orhan et al. 2019). Highly reliable information may be obtained from lake sediments by means of high-resolution geochemical data. Recently in many studies, the X-ray fluorescence (XRF) core scanning method has been used in obtaining high-resolution chemical data from core profiles (Boyle 2000; Koinig et al. 2003; Mayr et al. 2005; Martín-Puertas et al. 2011; Guimaraes et al. 2016; Zhao et al. 2016).

Konya Closed Basin has been studied by many workers because of its importance in geology, agriculture, and archeology (Roberts et al. 1979; Roberts 1983; Fontugne et al. 1999).

Although the Konya Closed Basin comprises Quaternary lake marls and other, mainly fine grained, sediments with locally in excess of 400 m, most of the works done in relation to the climatic and environmental changes were conducted on the coarse-grained marginal shoreline facies and associated landforms (beach ridges, wave-cut cliffs, etc.) which surround the plain and have the most obvious evidences of late Quaternary environmental changes (de Ridder 1965; Roberts 1983; Kuzucuoğlu et al. 1998; Fontugne et al. 1999; Karabıyıkoğlu et al. 1999; Roberts et al. 1999).

Present study has focused on the analysis of down-trench geochemical changes in fine grained lake sediments from the Konya paleolake in central Turkey. The aim of this paper is to present an integrated study using geochemical data including major, trace, and rare earth elements (REEs); elemental ratios; and age depth relation to reconstruct environmental and local climate changes of this region as well as depositional conditions during late Quaternary.

Study area

Konya Plain is an almost flat marl-filled former lake bottom having the altitude of which does not vary much around 1000 m, with lowest depressions at ca. 997 m. It covers an area of about 4200 km^2 and is located north of the Taurus ranges and south of the Tuz Gölü (Salt Lake) basin. It is separated from the Tuz Gölü drainage area by a pass only 50-m high, while the southern mountains rise up to over 3000 m. It is surrounded by the mountain Bozdağ (a Paleozoic limestone palaeorelief with heights points of 1500 m) to the northwest and two stratovolcanoes higher than 2000 m: the Pliocene andesitic Karacadağ to the northeast and the Pleistocene differentiated Karadağ to the south (Fig. 1a).

Materials and methods

Fifty-one samples about 10 cm apart were collected from a 7-m-deep trench (Adakale trench; 37.51198° N, 33.05998° E, Altitude: 1003 m) opened near the Adakale village (Fig. 1b). All of these samples were analyzed for their major oxides and trace elements including REEs. About 0.2 g of powdered samples from each sample was analyzed by inductively coupled plasma emission spectrometry (ICP-ES; major elements) and inductively coupled plasma mass spectrometry (ICP-MS; trace elements including REEs), in the Acme Analytical Laboratory (Vancouver, Canada). After lithium borate fusion, precision and accuracy were checked by parallel analysis of international reference standards. The minimum detection limit for major and minor elements is 0.01% while for trace element is 0.01 to 1 ppm.

Mollusk shells in three highly fossiliferous samples collected at depth of 60 cm, 419 cm, and 491 cm from the Adakale trench were dated by electron spin resonance (ESR) dating method which is based on measurements of the number of paramagnetic centers produced by natural radiation in a material (Ikeya 1993; Grün 1989; Blackwell et al. 2016). Equivalent doses (D_E) representing the accumulated natural radiation doses were obtained by means of the additive dose method. Annual dose rates (D) were determined using the natural radioactive element (^{238}U, ^{232}Th, ^{40}K) concentrations, cosmic dose rate contribution, grain sizes of powders, and moisture effect. ESR ages of the fossil shell samples were calculated taking into account of uranium uptake history of shells using ROSY program (Brennan et al. 1999). ESR spectra of the samples were recorded at room temperature by JEOL JESFa-300 X-band ESR spectrometer located at Selçuk University Advanced Technology Research & Application Center, Turkey.

Results

Major oxides

Ternary plot of major oxide (SiO_2, Al_2O_3, and CaO) content shows that most of samples are enriched in CaO relative to Al_2O_3 and SiO_2 (Table 1 and Fig. 2). Almost half of samples were identified as marl and the rest as limestone (Fig. 2). Fe_2O_3, TiO_2, and K_2O contents are generally relatively higher

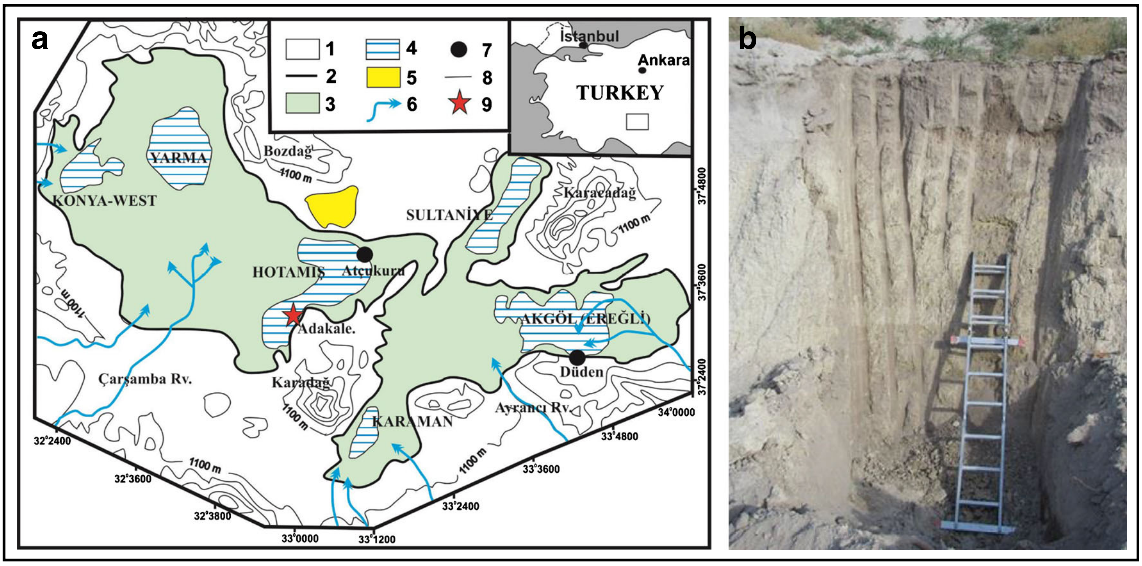

Fig. 1 **a** Map of the Upper Pleistocene Lake systems in the Konya Closed Basin (Fontugne et al.1999). 1 Limestone and volcanic basement. 2 Limit of Pleniglacial paleobeaches and fans. 3 Extension of Pleniglacial lake. 4 Approximate extension of Late Glacial and Holocene lakes and marshes. 5 İsmil dune system (Lake Glacial). 6 Main surface inflow. 7 Swallow holes. 8 Contours. 9 Sampling site (Adakale). **b** The appearance of a 7-m-deep trench

in samples having high SiO_2 and Al_2O_3, which are contributed to the high detrital input. MnO content is relatively low in those samples with high CaO which suggest anoxic bottom water conditions at the deposition time. There is a high positive correlation between SiO_2 and Al_2O_3, Fe_2O_3, MgO, K_2O, and TiO_2, whereas there is a high negative correlation between CaO and SiO_2, Al_2O_3, Fe_2O_3, MgO, K_2O, and TiO_2 (Table 2).

Trace elements

The distribution of most of trace elements is closely related to the detrital content of samples. They are clearly enriched in sediments having high SiO_2 and Al_2O_3 (Tables 1, 3, and 4). The Rb contents of samples are variable ranging from 1.6 to 68 ppm. There is a high negative correlation between Rb and CaO and high positive correlation between CaO and Sr (Table 2).

The redox sensitive elements such as Th, Ni, V, Fe, Cs, and Ce are relatively enriched in samples having high SiO_2 and Al_2O_3. This points an oxic bottom water condition. On the other hand, the Mo content is relatively higher in samples with higher CaO content suggesting anoxic conditions (Tables 1 and 3).

Elements used as paleoproductivity proxy (Cu, Ni, Ba) are relatively depleted in samples having high CaO content reflecting high productivity (Tables 1 and 3).

Dating

Mollusk shells (*Bithynia tentaculata* for L8A24, *Valvata piscinalis* for L8A31 and L8A50 Fig. 3) were selected as dating materials. The signal intensity of freely rotating CO_2^- radical at g = 2.0007 was used to determine D_E of samples (Grün 1989). Dose response curves of signals were best fitted to a single exponential saturation function, y = a * exp(bx) + c, using the Y2Science ESR data processing program. ESR spectrum and fitted dose response curve for L8A24 mollusk shells are shown in Fig. 4, respectively. The parameters of fit functions, equivalent doses, annual dose rates, and ESR dates obtained from mollusk shells are given on Table 5.

Discussion

Lacustrine sediments have been used to elucidate the paleoecological and paleoenvironmental conditions under which they were deposited by means of different geochemical proxies (Lei et al. 2008; Martín-Puertas et al. 2011; Guimaraes et al. 2016; Zhao et al. 2016).

Detrital influx proxies

Al, Ti, and Zr contents and Ca/Al, Ca/Ti, Si/Al, Ti/Al, and Sr/Al ratios have been widely used as detrital influx proxies (Murphy et al. 2000; Tribovillard et al. 2006; Zhao et al. 2016). In a place where climatic conditions prevailed by strong rainfall, erosion rate and detrital input to lakes will be high (de Oliveira et al. 2009). Al, Ti, and Zr content of these sediments will be high, while Ca/Al, Ca/Ti, and Sr/Al ratios will be low (Guimaraes et al. 2016; Zhao et al. 2016). Si in lacustrine sediments may be derived from both detrital and biogenic sources (Kidder and Erwin 2001). Zhao et al.

Table 1 Major oxide contents (in %) of the studied samples

Sample no	Depth (m)	SiO_2 %	Al_2O_3 %	FeO_2 %	MgO %	CaO %	Na_2O %	K_2O %	TiO_2 %	MnO %
L8A1	-6.81	28.62	6.45	3.31	2.47	28.32	0.58	1.17	0.38	0.05
L8A2	-6.71	23.86	4.93	1.96	2.20	33.26	0.55	0.94	0.31	0.05
L8A3	-6.63	26.67	5.05	2.00	1.97	31.63	0.64	0.95	0.30	0.04
L8A4	-6.56	31.10	5.52	2.21	1.80	29.15	0.68	1.02	0.32	0.03
L8A5	-6.51	34.46	5.27	1.32	1.48	28.99	1.03	0.96	0.26	0.03
L8A6	-6.46	34.76	5.00	1.26	1.49	29.22	0.99	0.91	0.29	0.03
L8A7	-6.39	33.07	4.79	1.29	1.60	30.08	0.88	0.84	0.32	0.03
L8A8	-6.31	29.40	4.53	1.64	1.69	31.61	0.73	0.79	0.28	0.03
L8A9	-6.25	27.88	4.66	1.70	1.77	32.38	0.72	0.84	0.28	0.03
L8A10	-6.15	25.21	4.07	1.36	1.69	34.57	0.68	0.74	0.26	0.03
L8A11	-6.05	25.34	4.13	1.23	1.68	34.66	0.69	0.74	0.26	0.03
L8A12	-5.95	22.02	3.64	1.16	1.75	36.83	0.61	0.63	0.23	0.03
L8A13	-5.85	16.29	2.96	0.99	1.77	40.69	0.48	0.48	0.18	0.03
L8A14	-5.75	14.32	2.85	0.93	1.74	41.96	0.42	0.45	0.17	0.02
L8A15	-5.69	18.61	3.41	1.02	1.77	39.03	0.52	0.55	0.21	0.03
L8A16	-5.63	19.36	3.60	1.10	1.86	38.05	0.57	0.61	0.22	0.03
L8A17	-5.61	5.88	1.38	0.53	1.29	46.32	0.21	0.21	0.07	< 0.01
L8A18	-5.51	1.06	0.22	0.17	0.97	53.00	0.08	0.05	0.02	< 0.01
L8A19	-5.41	1.90	0.42	0.23	0.76	52.51	0.11	0.08	0.03	< 0.01
L8A20	-5.31	3.45	0.79	0.33	0.90	51.40	0.14	0.13	0.05	< 0.01
L8A21	-5.21	4.13	0.96	0.44	1.14	50.26	0.16	0.17	0.06	< 0.01
L8A22	-5.11	5.75	1.49	0.48	0.88	49.55	0.18	0.22	0.07	< 0.01
L8A23	-5.01	3.55	0.83	0.36	0.83	51.39	0.13	0.15	0.05	< 0.01
L8A24	-4.91	1.49	0.37	0.17	0.95	52.78	0.07	0.06	0.02	< 0.01
L8A25	-4.79	2.60	0.73	0.35	1.13	51.77	0.10	0.13	0.03	< 0.01
L8A26	-4.69	11.17	3.32	1.11	1.68	42.90	0.24	0.53	0.12	0.02
L8A27	-4.59	13.74	3.60	1.40	1.53	41.19	0.31	0.58	0.14	0.02
L8A28	-4.50	14.57	3.14	1.26	1.50	41.60	0.33	0.52	0.15	0.02
L8A29	-4.40	25.44	4.16	1.01	1.49	35.31	0.75	0.73	0.20	0.02
L8A30	-4.28	22.50	3.77	1.00	1.54	37.38	0.64	0.66	0.22	0.02
L8A31	-4.19	11.91	2.06	0.48	1.24	44.9	0.37	0.27	0.09	0.02
L8A32	-4.06	19.99	3.53	1.00	1.29	39.07	0.49	0.62	0.25	0.02
L8A33	-3.98	2.99	0.32	0.30	0.77	52.18	0.07	0.05	0.02	< 0.01
L8A34	-3.79	1.74	0.22	0.22	0.92	53.24	0.06	0.04	0.02	0.02
L8A35	-3.66	39.86	7.06	2.00	2.02	23.78	0.86	1.18	0.55	0.03
L8A36	-3.56	37.79	8.24	2.95	3.17	21.41	0.70	1.44	0.50	0.03
L8A37	-3.46	37.31	8.19	2.73	3.36	21.71	0.70	1.42	0.51	0.03
L8A38	-3.26	39.40	8.29	2.56	3.04	21.08	0.81	1.43	0.55	0.04
L8A39	-3.06	39.44	8.18	2.67	2.68	21.59	0.79	1.39	0.54	0.04
L8A40	-2.86	37.76	7.98	2.97	3.25	21.81	0.75	1.36	0.51	0.05
L8A41	-2.66	38.46	7.86	2.55	3.33	21.72	0.78	1.33	0.53	0.05
L8A42	-2.46	39.28	7.47	2.66	2.85	22.23	0.85	1.25	0.56	0.05
L8A43	-2.26	36.19	7.37	2.92	3.39	23.00	0.72	1.25	0.50	0.05
L8A44	-2.06	31.93	7.88	2.99	3.74	24.25	0.58	1.34	0.46	0.06
L8A45	-1.86	34.05	7.46	2.81	3.2	24.41	0.68	1.24	0.47	0.06
L8A46	-1.56	31.49	7.23	2.67	3.44	25.71	0.62	1.19	0.44	0.06
L8A47	-1.26	31.96	6.96	2.70	3.06	25.91	0.61	1.17	0.44	0.06
L8A48	-1.06	31.13	6.79	2.64	2.87	26.97	0.62	1.17	0.44	0.06
L8A49	-0.80	11.54	2.72	0.95	1.97	43.64	0.29	0.46	0.16	0.02
L8A50	-0.60	5.68	1.45	0.37	1.36	49.17	0.24	0.31	0.06	0.01
L8A51	-0.10	1.91	0.47	0.27	1.37	52.23	0.09	0.09	0.03	< 0.01

(2016) stated that silica in siliceous and silty shales could possibly originate from biogenic sources which make silica or Si/Al ratios an unreliable indicator for detrital influx. Ti and K are typically associated with clays. Increase in Ti/K ratio infers high amounts of weathered clay minerals deposited during high water stands and wetter periods (Hodell et al. 2008). Zr and Hf are typically fixed in resistant minerals such as zircon, and thus an increase in these elements can provide an indication of high-energy terrestrial runoff in the basin (Guimaraes et al. 2016). Even though the usage of REEs in lacustrine sediments as paleoenvironmental indicators is not common, they have potential to be used as paleoenvironmental proxies, because they are sensitive to pH and salinity, redox fluctuations, and changes in detrital sources (Martín-Puertas 2011).

Table 2 **Correlation** coefficient matrix of variable pairs in the studied samples

	SiO_2	Al_2O_3	Fe_2O_3	MgO	CaO	Na_2O	K_2O	TiO_2	P_2O_5	MnO	Cr_2O_3	Ba	Ni	Cs	Ga	Hf	Rb	Sr	Th	U	V	Zr	Ce	Mo	Cu	Ni
SiO_2	**1.0**	.962	.883	.801	-.990	.949	.967	.955	.845	.798	.894	.902	.740	.826	.919	.907	.921	-.629	.952	.047	.899	.911	.932	-.208	.787	.814
Al_2O_3	.962	1.00	.962	.915	-.988	.839	.997	.983	.837	.857	.860	.906	.868	.891	.982	.864	.990	-.671	.990	.028	.971	.865	.976	-.219	.832	.925
Fe_2O_3	.883	.962	1.00	.931	-.934	.715	.961	.941	.787	.895	.770	.817	.915	.893	.956	.763	.977	-.662	.953	-.010	.960	.761	.931	-.176	.822	.948
MgO	.801	.915	.931	1.00	-.870	.616	.902	.902	.782	.879	.733	.759	.935	.808	.924	.730	.934	-.621	.915	-.027	.933	.731	.911	-.259	.807	.959
CaO	-.990	-.988	-.934	-.870	1.00	-.904	-.990	-.976	-.853	-.844	-.880	-.905	-.812	-.869	-.956	-.890	-.962	.644	-.978	-.054	-.944	-.893	-.959	.191	-.829	-.882
Na_2O	.949	.839	.715	.616	-.904	1.00	.851	.826	.767	.673	.830	.837	.519	.704	.760	.852	.764	-.469	.821	.092	.738	.858	.799	-.131	.677	.620
K_2O	.967	.997	.961	.902	-.990	.851	1.00	.978	.841	.852	.844	.908	.859	.896	.977	.852	.987	-.657	.988	.049	.964	.854	.973	-.191	.842	.916
TiO_2	.955	.983	.941	.902	-.976	.826	.978	1.00	.883	.848	.903	.872	.877	.842	.974	.915	.970	-.717	.992	.054	.968	.916	.979	-.226	.817	.921
P_2O_5	.845	.837	.787	.782	-.853	.767	.841	.883	1.00	.738	.832	.715	.734	.697	.810	.844	.814	-.582	.874	.089	.817	.852	.874	-.168	.758	.796
MnO	.798	.857	.895	.879	-.844	.673	.852	.848	.738	1.00	.699	.663	.852	.725	.834	.698	.859	-.550	.855	-.046	.851	.699	.819	-.215	.697	.858
Cr_2O_3	.894	.860	.770	.733	-.880	.830	.844	.903	.832	.699	1.00	.771	.675	.683	.830	.947	.812	-.674	.871	.036	.825	.950	.867	-.295	.644	.742
Ba	.902	.906	.817	.759	-.905	.837	.908	.872	.715	.663	.771	1.00	.669	.841	.874	.820	.884	-.449	.887	.100	.860	.822	.887	-.188	.773	.753
Ni	.740	.868	.915	.935	-.812	.519	.859	.877	.734	.852	.675	.669	1.00	.714	.915	.662	.903	-.748	.883	-.005	.902	.661	.871	-.202	.721	.966
Cs	.826	.891	.893	.808	-.869	.704	.896	.842	.697	.725	.683	.841	.714	1.00	.854	.704	.911	-.423	.863	.126	.886	.702	.850	-.042	.869	.811
Ga	.919	.982	.956	.924	-.956	.760	.977	.974	.810	.834	.830	.874	.915	.854	1.00	.825	.987	-.729	.976	.036	.972	.825	.963	-.225	.806	.951
Hf	.907	.864	.763	.730	-.890	.852	.852	.915	.844	.698	.947	.820	.662	.704	.825	1.00	.816	-.602	.888	.089	.834	.998	.886	-.264	.702	.735
Rb	.921	.990	.977	.934	-.962	.764	.987	.970	.814	.859	.812	.884	.903	.911	.987	.816	1.00	-.664	.981	.043	.981	.816	.969	-.201	.844	.949
Sr	-.629	-.671	-.662	-.621	.644	-.469	-.657	-.717	-.582	-.550	-.674	-.449	-.748	-.423	-.729	-.602	-.664	1.00	-.692	.159	-.667	-.597	-.678	.261	-.370	-.713
Th	.952	.990	.953	.915	-.978	.821	.988	.992	.874	.855	.871	.887	.883	.863	.976	.888	.981	-.692	1.00	.038	.969	.890	.991	-.230	.830	.931
U	.047	.028	-.010	-.027	-.054	.092	.049	.054	.089	-.046	.036	.100	-.005	.126	.036	.089	.043	.159	.038	1.00	.118	.087	.024	.683	.237	.086
V	.899	.971	.960	.933	-.944	.738	.964	.968	.817	.851	.825	.860	.902	.886	.972	.834	.981	-.667	.969	.118	1.00	.834	.956	-.142	.843	.948
Zr	.911	.865	.761	.731	-.893	.858	.854	.916	.852	.699	.950	.822	.661	.702	.825	.998	.816	-.597	.890	.087	.834	1.00	.889	-.267	.703	.733
Ce	.932	.976	.931	.911	-.959	.799	.973	.979	.874	.819	.867	.887	.871	.850	.963	.886	.969	-.678	.991	.024	.956	.889	1.00	-.265	.817	.920
Mo	-.208	-.219	-.176	-.259	.191	-.131	-.191	-.226	-.168	-.215	-.295	-.188	-.202	-.042	-.225	-.264	-.201	.261	-.230	.683	-.142	-.267	-.265	1.00	.033	-.131
Cu	.787	.832	.822	.807	-.829	.677	.842	.817	.758	.697	.644	.773	.721	.869	.806	.702	.844	-.370	.830	.237	.843	.703	.817	.033	1.00	.807
Ni	.814	.925	.948	.959	-.882	.620	.916	.921	.796	.858	.742	.753	.966	.811	.951	.735	.949	-.713	.931	.086	.948	.733	.920	-.131	.807	1.00

Enrichment in the elements (Al, K, Ti, Fe, REEs) which are associated with aluminosilicates points an increase in detrital input and high water level. But depletion in these elements is interpreted as a sign of low detrital input pointing a relatively dry climate which is characterized by weak erosion. Sediments deposited under this condition are carbonates and evaporates which are characterized by enrichment in Sr and S (Guimaraes et al. 2016). The changes in the Rb/Sr ratio reflect the rate of the chemical weathering of the rocks surrounding the lake in relation with the climate. Higher Rb/Sr ratio points a climate under which the chemical weathering is weak (Lei et al. 2008).

Si, Al, K, Ti, Ca, Fe, and ∑REEs contents as well as the Ti/Al, Rb/Sr, and Si/Ti ratios change systematically through the sampled section as shown in Fig. 5. The Si/Ti ratio is almost constant at the levels where the content of Si+Al+K+Ti+Fe is high and Ca content is low (Fig. 5). The two phases of enhanced Si/Ti (the periods III and IV) coincide with high Ca content. This has been contributed to the biogenic silica, because Si/Ti ratio is used an indicator of biogenic silica, which is linked to the changes in productivity of diatoms and sponges (Guimaraes et al. 2016; Sahoo et al. 2015)

Three levels correspond relatively to high Si, Al, K, Ti, Fe, and ∑REEs; low Ca contents; and high Ti/Al and Rb/Sr and low Si/Ti ratios. These levels represent periods of high detrital input. Three levels interbedded with them are characterized by relatively low Si, Al, K, Ti, Fe, and ∑REEs; high Ca contents; and lower Ti/Al and Rb/Sr and higher Si/Ti ratios (Fig. 5). These levels represent periods of low detrital input.

Six periods of detrital inputs were defined by means of the detrital influx proxies for the studied sediments (Fig. 5). The detrital input was high during periods I, III, and V. During these periods, a wet and cold climate was effective in the area; the erosion rate and the water level was high. On the other hand, periods II, IV, and VI are represented by low detrital input. During these periods, a hot and dry climate was effective in the area; the erosion rate and the water level was low.

Redox proxies

The concentration of redox sensitive elements such as U, Th, Mo, Ni, V, and Fe and trace element ratios may provide important clues about the paleoredox conditions. Most of the redox-sensitive trace metals tend to be more soluble under oxidizing conditions than under reducing conditions. This behavior makes U, V, and Mo and to a lesser extent certain other trace metals such as Cr and Co useful as paleoredox proxies. The combined use of U, V, and Mo enrichments may allow

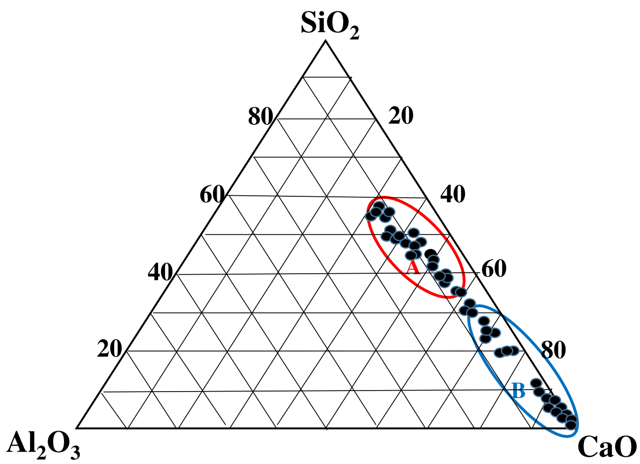

Fig. 2 Ternary diagram of major oxides of the studied samples (a Marl; b limestone)

suboxic environments to be distinguished from anoxic-euxinic ones (Tribovillard et al. 2006). Thorium is usually enriched in sediments deposited under oxic conditions (Wignall and Twitchett 1996), whereas aqueous U will be trapped by organic-rich sediments under reducing conditions (Kochenov et al. 1977). Therefore, high Th/U ratios point oxic conditions. Ni and V are adsorbed by organic matter under anoxic conditions (Lewan and Maynard 1982; Breit and Wanty 1991; Zhao et al. 2016), but the concentrations of Co and Cr are independent from redox conditions. High Ni/Co, V/Cr, and V/(V+Ni) values are considered to be resulted under anoxic conditions (Jones and Manning 1994; Zhao et al. 2016).

Four levels which are characterized by high Th, Ni, V, Cs, and Ce and low Mo contents were identified through the measured section (Table 3). Samples from these levels are also relatively enriched in SiO_2 and Al_2O_3 (Table 1), which point oxic bottom water condition.

Based on the redox proxies obtained from the studied samples, eight redox periods were distinguished (Fig. 6). The majority of redox proxies for periods I, III, V, and VII consistently reflect the oxygenated redox condition (high Mn, Th/U and low Ni/Co, Mo/Al and V/Cr; Fig. 6), whereas V/(V + Ni) ratios point to the anoxic condition. These periods correspond to increased fresh water input, high water stands, and well oxygenated, highly energetic bottom conditions. Periods II, IV, VI, and VIII are characterized by redox proxies of reduced condition (low Mn and Th/U and high Ni/Co, Mo/Al and V/Cr; Fig. 6). These periods correspond to periods of high evaporation, low water stands, and anoxic and stagnant bottom conditions.

Paleoproductivity proxies

Productivity of organisms in a lacustrine environment is controlled by the chemistry, temperature, salinity and turbidity of lake water, and terrigenous input. Several proxies such as Cu/Al, Ni/Al, Ca/Al, Ba/Al Si/Ti, and Ca/Ti have been used to predict the paleoproductivity.

Ni and Cu in sediments are mainly deposited first as organometallic complexes (Fernex et al. 1992; Algeo and Maynard 2004; Piper and Perkins 2004). Sediments bearing organometallic complexes matter generally degrade after deposition, but the released Ni and Cu may be incorporated into sediments under reducing conditions. Therefore, Ni and Cu may be used as reliable productivity indicators.

Ba is considered a paleoproductivity proxy since the biogenic barite is related to the phytoplankton decay (Dymond et al. 1992; Francois et al. 1995; Monnin et al. 1999; Jeandel et al. 2000). Schnetger et al. (2000) showed that the Ba/Al ratio in a sediment may be used as a reliable indicator for paleoproduction. Silica in lacustrine sediments may be derived from either detrital or biological sources so that the changes in the Si/Ti ratio in a sediment sequences have been used as an indicator of changes in the diatom and sponge productions (Hermanowski et al. 2012; Sahoo et al. 2015).

Elements of paleoproductivity proxies change systematically through the measured section. There is a highly negative correlation between CaO and the elements used in the interpretation of paleoproductivity (Table 1). Four levels which are relatively depleted in Cu, Ni, and Ba and enriched in CaO were determined within the studied samples. These levels represent high productivity periods.

Eight paleoproductivity periods were distinguished (Fig. 7) by means of commonly used proxies; periods I, III, V, and VII are represented by low paleoproductivity condition (low Cu/Al, Ni/Al, Ca/Al, Ba/Al Si/Ti, and Ca/Ti), while periods II, IV, VI, and VIII are characterized by high paleoproductivity condition (high Cu/Al, Ni/Al, Ca/Al, Ba/Al Si/Ti, and Ca/Ti).

Cold and wet climate is generally characterized by dense physical weathering and high erosion rate, which contribute high amount of detrital material to depositional sites, and by low productivity. This type of climate also causes deep ventilation of lake water and bottom water oxygenation. Contrarily, the hot and dry climate is generally represented by low weathering and erosion rates and high productivity. Under this climate, lake water is mainly stratified which resulted in a reduced bottom condition.

Low detrital input has been interpreted as an evidence for less erosive rainfall events and/or high catchment stability, possibly indicating a drier period. This could be supported by an increase in Ca precipitation (higher Ca/Al) and high detrital organic matter content (Martín-Puertas 2011).

Periods represented by high detrital input, low productivity, and oxic bottom condition are interpreted as being products of cold and wet climate, while periods characterized by low detrital input, high productivity, and anoxic bottom condition are considered results of cold and wet climate. Levels determined by using paleoenvironmental and paleoecological

Table 3 Trace elements content (in ppm) of the studied samples

Sample no	Depth (m)	Ba	Ni	Co	Cs	Ga	Hf	Nb	Rb	Sr	Ta	Th	U	V	W	Zr	Mo	Cu	Pb	Zn	Ni	As	La	Ce	Pr	Nd	Sm	Eu
L8A1	-6.81	358	40	8.8	11.3	6.0	2.1	9.0	53.3	832.9	0.6	6.7	2.5	58	0.7	80.8	1.6	7.4	10.2	20	34.5	3.1	19.2	35.3	3.94	14.7	2.49	0.65
L8A2	-6.71	345	36	6.9	9.5	4.8	2.1	6.8	41.7	1518.0	0.4	5.6	4.1	48	0.9	85.0	1.6	11.9	8.7	18	27.4	5.7	16.2	30.7	3.44	12.4	2.24	0.51
L8A3	-6.63	344	32	6.1	10.9	4.2	2.5	6.0	42.2	1414.0	0.3	5.3	3.6	40	0.7	96.7	1.7	12.8	7.9	19	25.8	5.6	15.5	27.8	3.14	11.4	2.05	0.47
L8A4	-6.56	336	30	6.0	11.0	5.2	2.4	6.5	44.5	1003.9	0.5	5.5	2.7	51	1.1	93.2	0.4	9.6	7.4	15	22.7	4.2	16.6	29.5	3.40	12.3	2.30	0.61
L8A5	-6.51	382	23	5.2	6.6	4.3	2.3	5.0	32.4	943.8	0.4	4.8	2.6	33	< 0.5	88.4	1.0	6.3	3.7	10	17.0	5.3	12.7	24.4	2.56	10.2	1.70	0.48
L8A6	-6.46	380	20	4.7	5.8	4.3	3.5	6.1	30.9	956.2	0.4	4.6	2.5	33	< 0.5	136.6	0.7	4.9	3.4	9	15.5	4.7	14.0	26.9	2.91	11.3	2.02	0.54
L8A7	-6.39	359	< 20	4.5	6.2	3.9	3.9	6.6	30.6	1000.0	0.4	5.0	2.3	33	0.9	164.7	0.5	5.0	3.4	9	14.0	4.6	15.3	29.3	3.12	11.8	2.08	0.53
L8A8	-6.31	284	23	4.7	7.3	3.6	3.7	5.4	31.1	1114.0	0.3	4.7	2.1	31	0.9	140.5	0.3	6.5	4.0	10	14.3	4.8	13.6	26.0	2.86	11.3	2.03	0.46
L8A9	-6.25	313	24	5.3	8.6	4.0	3.1	5.5	35.1	1146.9	0.4	4.4	2.7	40	0.9	122.1	1.0	11.2	5.2	14	19.4	6.1	13.6	24.1	2.81	10.1	1.94	0.46
L8A10	-6.15	327	26	5.0	7.1	3.4	3.1	5.3	29.1	1322.0	0.4	4.0	3.6	34	0.5	126.9	0.7	8.4	4.0	11	17.1	6.7	12.5	23.9	2.64	9.8	1.72	0.44
L8A11	-6.05	336	24	4.5	6.7	3.4	3.0	5.5	29.7	1298.4	0.3	4.0	3.6	40	0.6	125.0	0.9	6.9	3.9	10	15.6	6.9	12.5	23.8	2.61	9.6	1.69	0.44
L8A12	-5.95	343	< 20	4.3	7.0	3.0	3.3	4.8	26.1	1380.1	0.4	3.8	3.2	41	0.7	129.7	0.9	6.0	3.5	12	14.7	6.4	12.4	22.5	2.46	9.3	1.68	0.40
L8A13	-5.85	291	< 20	3.7	6.0	1.8	2.6	3.8	20.4	1488.1	0.3	3.2	3.1	36	< 0.5	106.8	0.8	8.5	2.9	8	12.0	7.2	10.0	18.5	2.05	7.8	1.34	0.36
L8A14	-5.75	265	< 20	3.5	6.3	2.1	2.2	3.3	19.9	1515.1	0.2	2.6	2.8	28	< 0.5	82.0	0.9	9.2	2.7	9	12.5	7.0	8.6	16.1	1.80	6.7	1.24	0.31
L8A15	-5.69	256	< 20	4.4	7.1	2.1	3.2	4.5	23.3	1359.6	0.3	3.6	2.9	35	< 0.5	124.3	0.9	5.8	3.1	9	13.3	6.5	10.7	20.6	2.25	8.1	1.50	0.35
L8A16	-5.63	259	23	4.2	7.3	2.8	2.9	4.8	25.2	1411.3	0.4	3.5	3.3	36	0.6	118.8	1.1	5.7	3.5	9	14.7	7.3	11.0	19.8	2.26	8.2	1.62	0.39
L8A17	-5.61	128	23	1.6	3.8	1.3	0.6	1.9	9.2	1245.3	0.1	1.0	4.5	23	< 0.5	25.9	2.6	6.9	1.4	4	23.6	3.8	3.6	6.9	0.74	3.0	0.50	0.14
L8A18	-5.51	101	< 20	0.5	0.9	< 0.5	< 0.1	0.5	1.6	1053.5	< 0.1	< 0.2	2.7	9	< 0.5	5.4	1.2	1.0	0.2	1	5.6	2.0	0.9	1.4	0.08	0.5	0.05	0.04
L8A19	-5.41	88	< 20	0.7	1.7	< 0.5	0.3	0.7	3.5	939.2	< 0.1	0.5	4.6	15	< 0.5	9.9	1.3	1.5	0.5	2	10.8	2.0	1.9	2.8	0.22	1.1	0.12	0.05
L8A20	-5.31	122	< 20	0.7	3.3	0.7	0.4	1.2	6.8	1055.6	< 0.1	0.6	3.7	14	< 0.5	16.4	1.1	1.3	0.8	3	9.1	1.1	2.5	4.4	0.42	1.6	0.24	0.09
L8A21	-5.21	160	< 20	0.7	4.6	0.7	0.5	1.4	8.3	1261.8	< 0.1	0.9	2.7	17	< 0.5	19.5	1.2	2.1	1.1	4	9.3	2.2	3.5	7.1	0.65	2.6	0.48	0.09
L8A22	-5.11	160	< 20	1.2	5.6	1.3	0.7	1.8	11.6	1013.2	0.1	1.1	2.0	15	< 0.5	30.4	0.9	1.6	1.2	5	7.0	1.5	4.3	7.9	0.77	2.9	0.50	0.15
L8A23	-5.01	174	< 20	1.0	3.2	< 0.5	0.5	1.2	7.0	1059.6	< 0.1	0.5	2.6	16	< 0.5	18.1	1.1	2.0	0.8	3	6.6	2.0	3.1	4.7	0.43	1.7	0.24	0.08
L8A24	-4.91	144	< 20	0.3	1.0	< 0.5	0.1	0.3	3.0	1529.3	< 0.1	< 0.2	2.3	8	< 0.5	5.8	0.3	0.9	0.6	2	3.9	1.7	1.2	2.1	0.22	0.9	0.17	0.03
L8A25	-4.79	187	< 20	1.1	2.0	< 0.5	0.2	0.9	6.2	1242.2	< 0.1	0.4	2.4	14	< 0.5	11.1	0.6	1.9	0.8	4	5.4	2.5	2.1	3.3	0.30	1.5	0.19	0.05
L8A26	-4.69	433	< 20	3.0	8.6	3.2	0.8	3.0	29.9	1732.6	0.2	2.1	3.3	34	0.5	30.6	0.5	4.8	3.4	10	14.4	3.0	7.8	14.7	1.56	5.8	1.02	0.24
L8A27	-4.59	299	< 20	2.7	9.2	3.4	1.1	3.3	30.0	1454.8	0.2	2.7	2.1	31	0.7	39.4	0.6	6.4	3.6	10	15.8	2.5	8.8	17.2	1.80	7.1	1.20	0.30
L8A28	-4.50	261	< 20	2.7	7.4	2.5	1.7	3.6	23.3	1148.3	0.3	2.9	1.8	27	0.6	70.1	0.3	5.3	3.2	8	14.1	2.1	9.6	17.9	1.92	7.2	1.16	0.31
L8A29	-4.40	352	< 20	3.2	5.7	3.9	1.9	4.8	27.3	1223.1	0.2	3.7	2.7	25	0.6	75.9	0.4	4.6	3.2	8	14.1	2.6	11.2	21.3	2.25	8.9	1.46	0.41
L8A30	-4.28	329	< 20	3.5	6.2	3.2	3.0	5.1	25.4	1166.8	0.3	3.6	2.9	28	< 0.5	122.7	0.5	4.1	3.1	9	13.8	2.4	12.2	23.5	2.51	9.6	1.77	0.42
L8A31	-4.19	210	< 20	1.8	2.8	0.5	1.4	2.2	9.7	1136.0	0.1	1.8	1.6	19	< 0.5	57.9	0.2	2.1	2.0	4	6.6	2.6	6.2	12.2	1.33	4.8	0.98	0.24
L8A32	-4.06	255	< 20	3.3	8.1	3.3	3.0	5.5	27.2	894.4	0.4	3.6	2.4	33	0.7	113.6	0.5	5.8	3.2	10	13.2	4.1	12.6	23.4	2.47	9.6	1.74	0.41
L8A33	-3.98	105	< 20	1.6	1.1	< 0.5	0.1	0.4	2.3	1019.5	< 0.1	< 0.2	1.5	10	< 0.5	6.5	0.3	2.0	0.4	5	4.9	1.7	1.1	1.8	0.13	0.6	0.06	0.03
L8A34	-3.79	109	< 20	1.2	0.4	< 0.5	0.2	0.3	1.7	1061.9	< 0.1	< 0.2	2.2	< 8	< 0.5	6.7	0.3	2.7	0.2	4	4.6	2.2	0.8	1.6	0.07	0.5	< 0.05	< 0.02
L8A35	-3.66	473	35	6.7	8.6	7.3	7.9	11.6	53.1	685.0	0.7	8.7	3.6	61	1.3	297.2	0.2	8.1	7.0	22	31.3	3.2	26.0	50.6	5.54	21.3	3.80	0.83

Table 3 (continued)

Sample no	Depth (m)	Ba	Ni	Co	Cs	Ga	Hf	Nb	Rb	Sr	Ta	Th	U	V	W	Zr	Mo	Cu	Pb	Zn	Ni	As	La	Ce	Pr	Nd	Sm	Eu
L8A36	-3.56	476	47	8.0	12.6	8.9	3.8	11.7	67.6	644.0	0.7	8.5	3.1	74	1.5	151.2	0.5	13.3	9.1	28	40.7	3.8	26.6	52.4	5.45	20.8	3.42	0.82
L8A37	-3.46	486	45	7.8	12.8	9.1	4.2	12.1	68.0	678.5	0.8	8.7	3.2	76	1.4	169.6	0.9	13.0	9.4	28	41.7	4.0	26.4	51.7	5.69	21.4	3.78	0.82
L8A38	-3.26	507	43	9.9	10.8	8.8	5.0	12.1	65.0	619.6	0.7	8.9	3.3	75	1.1	190.8	1.2	12.0	9.0	27	40.2	3.9	26.4	51.6	5.49	21.1	3.64	0.88
L8A39	-3.06	539	47	8.5	10.3	8.9	4.8	11.7	64.2	590.8	0.7	9.2	2.6	67	1.1	195.3	0.5	10.8	9.2	28	39.9	4.2	26.2	50.6	5.53	20.3	3.56	0.84
L8A40	-2.86	469	50	9.2	9.9	8.2	4.7	11.4	61.3	656.1	0.8	8.4	2.5	63	0.9	178.6	0.4	9.5	8.5	27	40.4	7.6	25.2	48.7	5.34	18.9	3.65	0.81
L8A41	-2.66	399	48	10.2	9.7	8.4	4.7	11.3	59.4	651.3	0.8	8.1	2.7	66	1.1	185.8	0.3	11.9	8.6	25	41.9	6.7	24.8	47.5	5.07	18.8	3.22	0.76
L8A42	-2.46	368	43	8.8	8.4	7.4	6.2	11.1	53.7	631.6	0.7	8.3	2.6	65	1.1	245.6	0.3	10.1	7.5	22	37.4	7.0	25.2	48.8	5.29	19.9	3.65	0.86
L8A43	-2.26	458	46	10.3	10.0	7.8	5.1	10.6	57.1	661.9	0.8	8.1	2.2	65	1.4	200.3	0.2	11.1	8.5	25	44.0	19.6	23.6	45.0	5.00	18.7	3.45	0.77
L8A44	-2.06	367	53	11.2	11.2	8.2	3.5	10.7	66.4	697.1	0.7	8.2	2.5	67	1.3	135.3	0.3	11.3	10.2	26	47.4	9.9	25.1	46.8	5.17	18.4	3.52	0.77
L8A45	-1.86	361	47	10.2	9.6	7.1	4.7	10.4	58.0	702.6	0.6	7.7	2.2	65	0.9	174.4	0.2	8.0	8.6	22	40.6	8.7	23.9	45.8	5.06	19.0	3.52	0.73
L8A46	-1.56	368	48	9.8	8.7	7.9	3.5	9.6	56.9	740.4	0.6	7.7	2.2	63	1.0	133.1	0.1	8.5	8.6	23	41.8	9.6	21.9	42.1	4.55	17.2	3.26	0.73
L8A47	-1.26	318	45	8.9	9.0	7.5	3.3	9.9	57.2	734.5	0.6	7.3	2.3	61	1.0	135.4	0.1	7.4	8.7	22	40.7	13.0	21.8	41.0	4.64	17.9	3.15	0.74
L8A48	-1.06	293	47	8.2	8.4	7.1	2.9	9.4	56.1	701.1	0.5	7.2	2.1	61	1.1	120.2	0.2	6.8	8.9	21	36.9	9.7	21.4	39.9	4.42	16.7	2.94	0.73
L8A49	-0.80	197	< 20	3.5	7.7	1.5	1.4	3.6	21.3	1259.6	0.3	2.9	2.4	21	< 0.5	57.2	0.2	7.6	3.2	9	16.5	5.1	9.8	17.9	1.77	6.8	1.21	0.30
L8A50	-0.60	235	< 20	1.8	3.2	< 0.5	0.8	2.2	10.8	1482.8	0.1	2.5	2.1	12	< 0.5	38.1	0.2	4.1	4.4	5	11.2	2.3	18.7	26.6	2.36	7.2	0.89	0.24
L8A51	-0.10	143	< 20	1.7	1.9	< 0.5	0.2	0.7	3.5	1401.2	< 0.1	0.4	1.8	< 8	< 0.5	8.3	0.2	3.7	0.6	2	8.1	3.1	2.1	3.6	0.30	1.1	0.12	0.05

Table 4 Rare earth elements' (REEs) content (in ppm) of the studied samples

Sample no	Depth (m)	Y	La	Ce	Pr	Nd	Sm	Eu	Gd	Tb	Dy	Ho	Er	Tm	Yb	Lu
L8A1	-6.81	11.8	19.2	35.3	3.94	14.7	2.49	0.65	2.37	0.36	2.03	0.41	1.21	0.18	1.12	0.17
L8A2	-6.71	9.8	16.2	30.7	3.44	12.4	2.24	0.51	2.13	0.29	1.94	0.33	1.01	0.14	0.99	0.12
L8A3	-6.63	10.1	15.5	27.8	3.14	11.4	2.05	0.47	1.98	0.27	1.72	0.32	0.87	0.13	0.90	0.14
L8A4	-6.56	10.9	16.6	29.5	3.40	12.3	2.30	0.61	2.14	0.30	1.93	0.33	1.03	0.17	1.01	0.16
L8A5	-6.51	8.8	12.7	24.4	2.56	10.2	1.70	0.48	1.66	0.23	1.41	0.28	0.82	0.12	0.74	0.12
L8A6	-6.46	10.3	14.0	26.9	2.91	11.3	2.02	0.54	1.92	0.27	1.82	0.33	1.01	0.17	0.97	0.15
L8A7	-6.39	11.4	15.3	29.3	3.12	11.8	2.08	0.53	2.08	0.29	1.90	0.35	1.08	0.16	1.04	0.16
L8A8	-6.31	8.8	13.6	26.0	2.86	11.3	2.03	0.46	1.87	0.25	1.56	0.30	0.86	0.14	0.97	0.13
L8A9	-6.25	9.7	13.6	24.1	2.81	10.1	1.94	0.46	1.92	0.26	1.69	0.30	0.92	0.14	0.95	0.13
L8A10	-6.15	8.3	12.5	23.9	2.64	9.8	1.72	0.44	1.64	0.23	1.45	0.31	0.85	0.12	0.79	0.14
L8A11	-6.05	8.3	12.5	23.8	2.61	9.6	1.69	0.44	1.64	0.23	1.37	0.27	0.76	0.13	0.84	0.12
L8A12	-5.95	7.6	12.4	22.5	2.46	9.3	1.68	0.40	1.61	0.21	1.34	0.26	0.70	0.11	0.78	0.13
L8A13	-5.85	6.8	10.0	18.5	2.05	7.8	1.34	0.36	1.32	0.20	1.18	0.21	0.75	0.10	0.66	0.10
L8A14	-5.75	5.9	8.6	16.1	1.80	6.7	1.24	0.31	1.19	0.17	1.03	0.20	0.59	0.09	0.59	0.09
L8A15	-5.69	7.6	10.7	20.6	2.25	8.1	1.50	0.35	1.46	0.21	1.29	0.26	0.81	0.11	0.75	0.12
L8A16	-5.63	8.1	11.0	19.8	2.26	8.2	1.62	0.39	1.48	0.21	1.27	0.25	0.73	0.11	0.74	0.11
L8A17	-5.61	2.5	3.6	6.9	0.74	3.0	0.50	0.14	0.51	0.08	0.48	0.11	0.26	0.04	0.27	0.04
L8A18	-5.51	0.7	0.9	1.4	0.08	0.5	0.05	0.04	0.13	0.02	0.13	0.03	0.06	< 0.01	0.05	< 0.01
L8A19	-5.41	1.2	1.9	2.8	0.22	1.1	0.12	0.05	0.19	0.03	0.19	0.04	0.13	0.02	0.10	0.02
L8A20	-5.31	1.8	2.5	4.4	0.42	1.6	0.24	0.09	0.31	0.05	0.33	0.06	0.18	0.03	0.16	0.03
L8A21	-5.21	2.1	3.5	7.1	0.65	2.6	0.48	0.09	0.40	0.06	0.38	0.07	0.24	0.04	0.21	0.03
L8A22	-5.11	2.8	4.3	7.9	0.77	2.9	0.50	0.15	0.54	0.08	0.51	0.11	0.34	0.05	0.25	0.04
L8A23	-5.01	1.7	3.1	4.7	0.43	1.7	0.24	0.08	0.32	0.05	0.26	0.07	0.17	0.02	0.16	0.02
L8A24	-4.91	1.0	1.2	2.1	0.22	0.9	0.17	0.03	0.16	0.02	0.10	0.03	0.08	0.01	0.08	< 0.01
L8A25	-4.79	1.2	2.1	3.3	0.30	1.5	0.19	0.05	0.26	0.04	0.16	0.04	0.14	0.02	0.11	0.02
L8A26	-4.69	4.7	7.8	14.7	1.56	5.8	1.02	0.24	0.98	0.14	0.86	0.16	0.50	0.07	0.43	0.07
L8A27	-4.59	5.3	8.8	17.2	1.80	7.1	1.20	0.30	1.05	0.16	0.94	0.17	0.53	0.07	0.50	0.07
L8A28	-4.50	6.0	9.6	17.9	1.92	7.2	1.16	0.31	1.22	0.18	1.02	0.20	0.63	0.09	0.55	0.09
L8A29	-4.40	7.5	11.2	21.3	2.25	8.9	1.46	0.41	1.46	0.20	1.17	0.25	0.85	0.11	0.65	0.11
L8A30	-4.28	8.1	12.2	23.5	2.51	9.6	1.77	0.42	1.60	0.23	1.41	0.28	0.90	0.13	0.82	0.13
L8A31	-4.19	4.3	6.2	12.2	1.33	4.8	0.98	0.24	0.89	0.13	0.71	0.14	0.40	0.07	0.44	0.05
L8A32	-4.06	8.2	12.6	23.4	2.47	9.6	1.74	0.41	1.56	0.22	1.53	0.26	0.88	0.12	0.83	0.12
L8A33	-3.98	0.7	1.1	1.8	0.13	0.6	0.06	0.03	0.17	0.02	0.16	0.03	0.08	0.01	0.09	0.01
L8A34	-3.79	0.5	0.8	1.6	0.07	0.5	< 0.05	< 0.02	0.11	0.01	0.11	< 0.02	0.05	< 0.01	0.05	< 0.01
L8A35	-3.66	18.1	26.0	50.6	5.54	21.3	3.80	0.83	3.53	0.50	3.21	0.63	1.82	0.27	1.79	0.30
L8A36	-3.56	15.8	26.6	52.4	5.45	20.8	3.42	0.82	3.36	0.49	3.02	0.56	1.71	0.25	1.46	0.24
L8A37	-3.46	17.1	26.4	51.7	5.69	21.4	3.78	0.82	3.53	0.49	3.00	0.57	1.70	0.26	1.68	0.24
L8A38	-3.26	17.7	26.4	51.6	5.49	21.1	3.64	0.88	3.50	0.49	3.11	0.59	1.77	0.25	1.74	0.26
L8A39	-3.06	16.8	26.2	50.6	5.53	20.3	3.56	0.84	3.30	0.48	3.02	0.60	1.67	0.25	1.63	0.25
L8A40	-2.86	16.5	25.2	48.7	5.34	18.9	3.65	0.81	3.19	0.45	2.79	0.53	1.58	0.23	1.53	0.23
L8A41	-2.66	16.9	24.8	47.5	5.07	18.8	3.22	0.76	3.24	0.46	2.72	0.56	1.70	0.24	1.58	0.25
L8A42	-2.46	17.0	25.2	48.8	5.29	19.9	3.65	0.86	3.37	0.50	3.10	0.60	1.81	0.26	1.74	0.28
L8A43	-2.26	16.5	23.6	45.0	5.00	18.7	3.45	0.77	3.21	0.47	2.71	0.58	1.55	0.24	1.57	0.25
L8A44	-2.06	16.0	25.1	46.8	5.17	18.4	3.52	0.77	3.35	0.48	2.63	0.54	1.55	0.23	1.55	0.25
L8A45	-1.86	15.0	23.9	45.8	5.06	19.0	3.52	0.73	3.23	0.45	2.59	0.56	1.64	0.25	1.51	0.23
L8A46	-1.56	14.2	21.9	42.1	4.55	17.2	3.26	0.73	2.84	0.43	2.63	0.49	1.42	0.21	1.30	0.20
L8A47	-1.26	15.1	21.8	41.0	4.64	17.9	3.15	0.74	2.96	0.43	2.72	0.49	1.49	0.20	1.46	0.23
L8A48	-1.06	14.2	21.4	39.9	4.42	16.7	2.94	0.73	2.81	0.43	2.46	0.50	1.42	0.22	1.38	0.21
L8A49	-0.80	5.8	9.8	17.9	1.77	6.8	1.21	0.30	1.10	0.15	0.96	0.20	0.49	0.09	0.54	0.09
L8A50	-0.60	2.4	18.7	26.6	2.36	7.2	0.89	0.24	0.71	0.09	0.49	0.08	0.22	0.03	0.23	0.03
L8A51	-0.10	0.9	2.1	3.6	0.30	1.1	0.12	0.05	0.18	0.03	0.18	0.03	0.11	< 0.01	0.09	0.01

Table 5 ESR dating results of the studied samples

Sample no	The a, b, and c parameters of fitted function, y=a * exp(bx)+c, used to determine equivalent doses	Equivalent dose DE (Gy)	Annual dose D (mGy/a)	Date - T_{ESR} (years) (early uptake)
L8A24	-601.37; -0.00065; 614.79	33.90±3.42	0.81	42009±4239
L8A31	-239.92; -0.00176; 253.50	31.21±2.21	0.95	32819±2414
L8A50	-346.25; -0.00099; 353.91	22.05±1.45	0.87	25276±1732

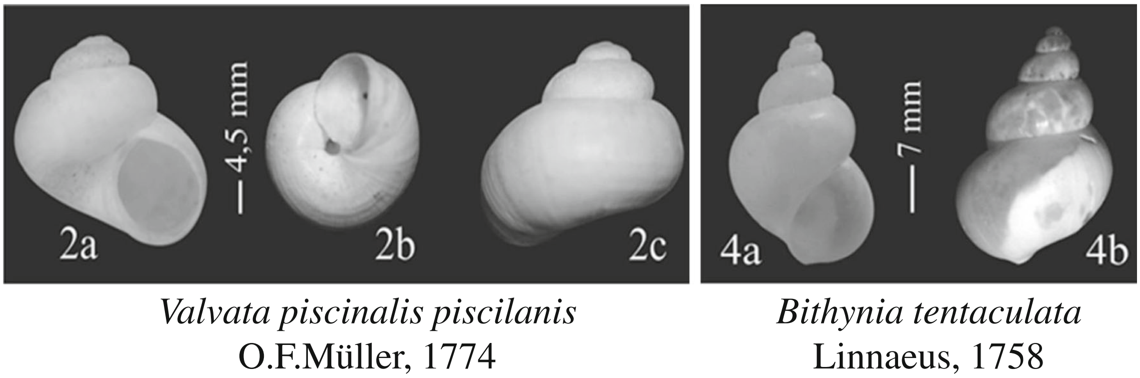

Fig. 3 Mollusca shells used for ESR dating

proxies on the studied samples are quite compatible with each other (Fig. 8). Interpretation done from all levels defined by different proxies almost confirm each other.

Climatic records

Global climate during the last glacial (~ 120 ka–10 ka before present) period has experienced at least twenty short-lived abrupt and large-amplitude warming shifts called Dansgaard-Oeschger (D/O) events determined in Greenland ice cores (Rahmstorf 2002; Rahmstorf 2003; Lowe and Walker 1997). These events are not local to Greenland. They have also been recorded in many other places (Rahmstorf 2002). D/O events start with a rapid warming by 5–10 °C within at most a few decades, followed by a plateau phase with slow cooling lasting several centuries, then a more rapid drop back to cold staidly conditions (Fig. 9; Johnsen et al. 1992; Dansgaard et al. 1993; Rahmstorf 2002). Heinrich events (H) are the second major type of climatic event that occurred mostly in the latter half of the last glacial. They are the coldest intervals between D/O events (Fig. 9; Rahmstorf 2002).

The geochemical data obtained from the late Quaternary lacustrine sediment of the Great Konya lake on the Adakale trench close to Adakale village (Konya, central Anatolia) show considerable variability over the past 50 ka, which coincide to the last half of the glacial periods. Climate during the last glacial period was not stable; two differing types of climates had been effectively repeated which can be interpreted in terms of changes in palaeohydrology and paleoclimate conditions.

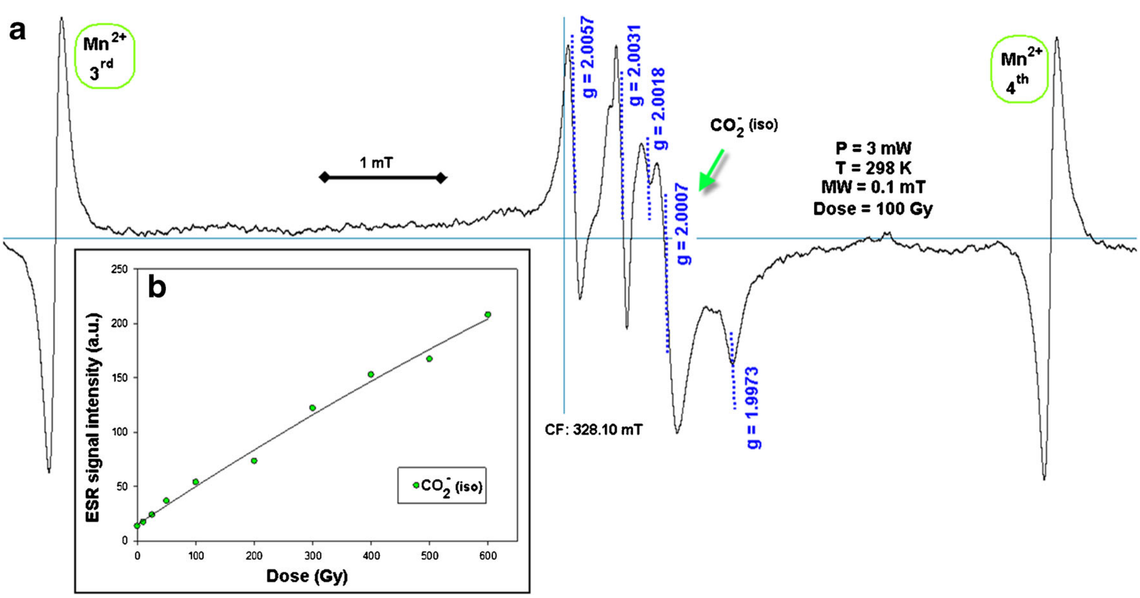

Fig. 4 **a** ESR spectrum of 100 Gy irradiated L8A24 mollusk shells. **b** Dose response curve of CO_2^- signal (g = 2.0007) observed in L8A24 mollusk shells

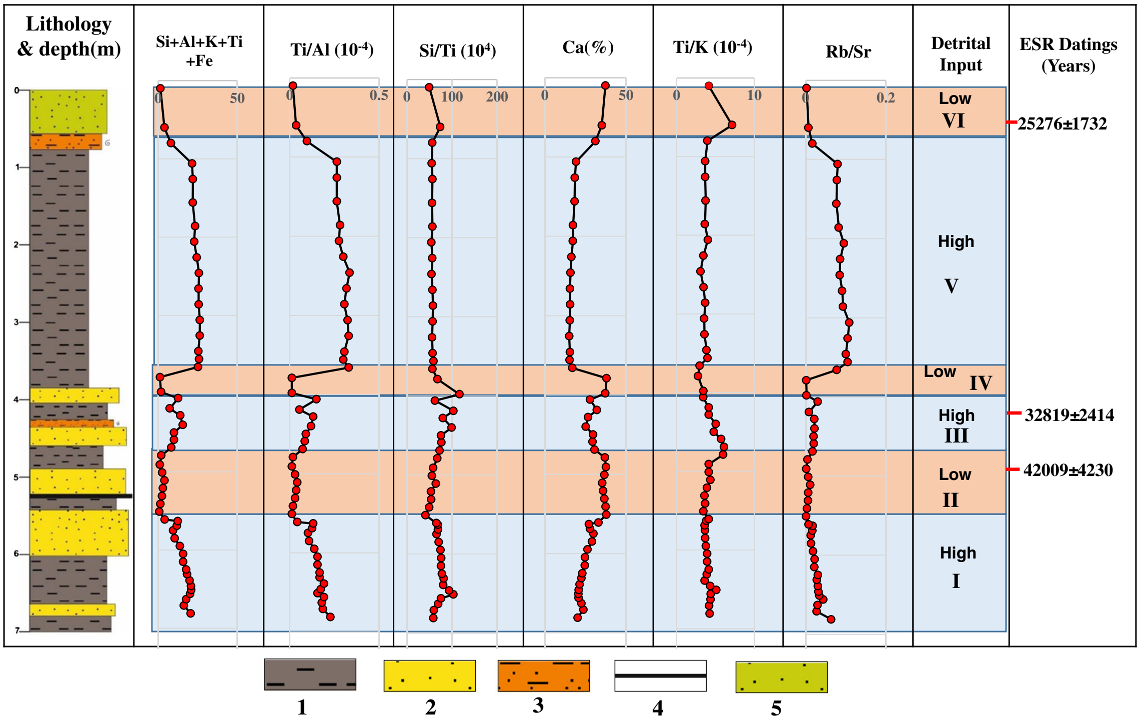

Fig. 5 The down trench distribution of detrital influx proxies; 1 mudstone; 2 fine sandy silt; 3 silty clayey fine sand; 4 organic rich mud; 5 organic rich fine sand

Four relatively cold climate periods and four relatively hot periods were interpreted from geochemical data of the studied samples (Fig. 8). Their approximated duration and corresponding events are given on Fig. 9.

Conclusions

Detailed geochemical analysis of samples taken from a 7-m-deep Adakale trench from the late Quaternary lacustrine

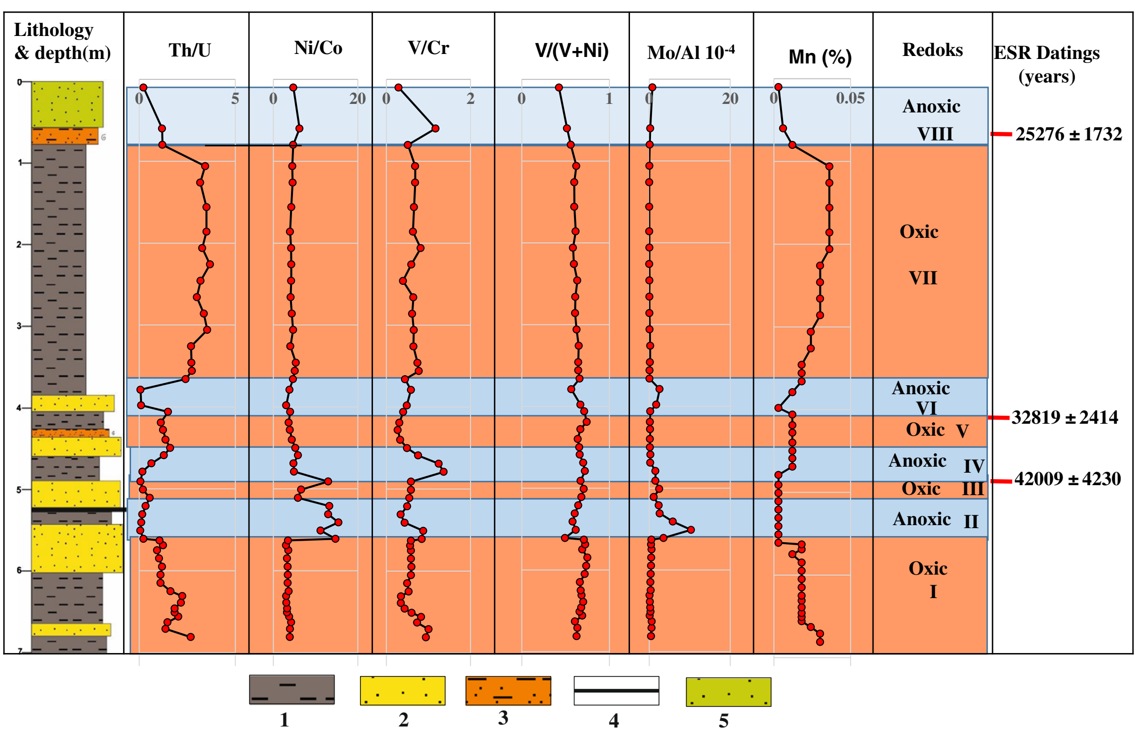

Fig. 6 The down trench distribution of redox proxies; 1 mudstone; 2 fine sandy silt; 3 silty clayey fine sand; 4 organic rich mud; 5 organic rich fine sand

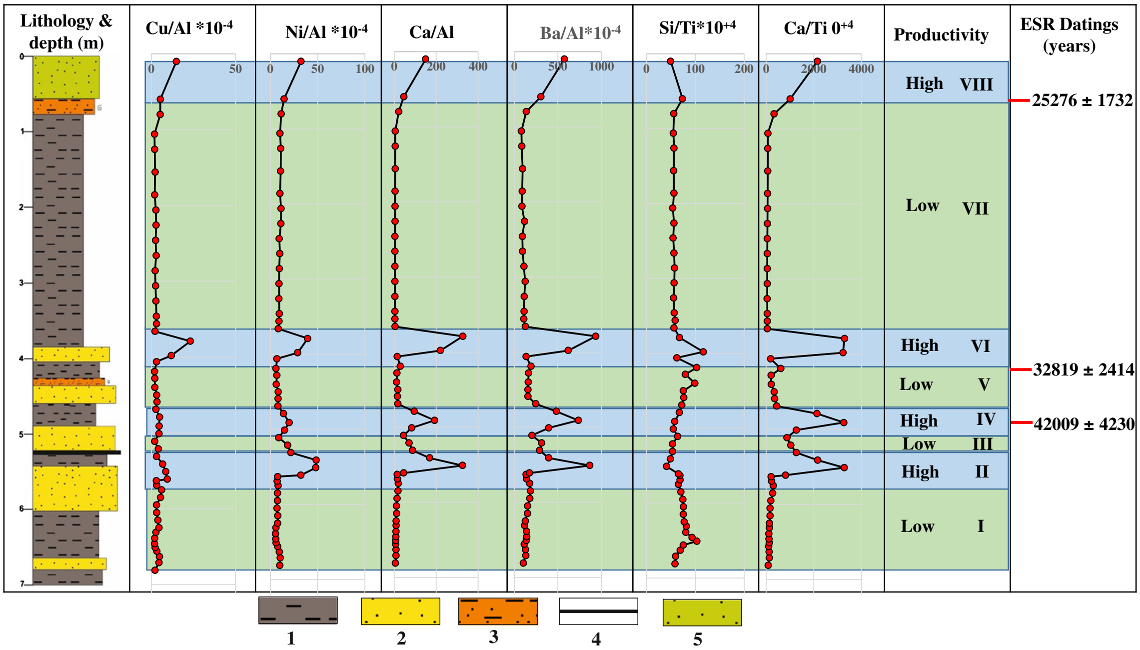

Fig. 7 The down trench distribution of productivity proxies; 1 mudstone; 2 fine sandy silt; 3 silty clayey fine sand; 4 organic rich mud; 5 organic rich fine sand

sediments in the Konya Closed Basin, central Anatolia, provides important information about climatic changes and hydrological conditions in the area during late Quaternary. Climate changes observed during last 50 ka were represented by oscillations in weathering processes, detrital input, redox conditions, water levels, and paleoproductivity in the studied lakes.

Three periods of high detrital input (high Si+Al+K+Ti+Fe, high Ti/Al, Rb/Sr, low Ca and low Si/Ti), four periods of anoxic conditions (low Mn, Th/U and high Ni/Co, Mo/Al and V/Cr), and four periods of higher productivity (high Cu/Al, Ni/Al, Ca/Al, Ba/Al Si/Ti and Ca/Ti) were identified from the study area by using geochemical data. These periods are considered to be resulted from climatic changes during last

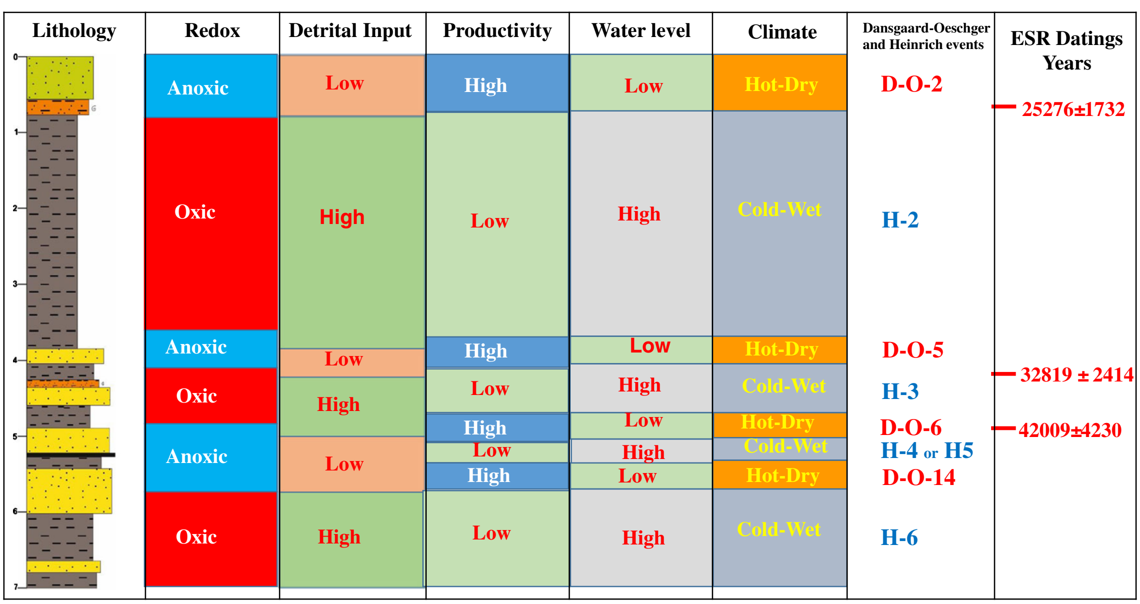

Fig. 8 The interrelation among the climate, water level determined by paleoenvironmental and paleoecological proxies, Dansgaard-Oeschger, and Henrich climatic events

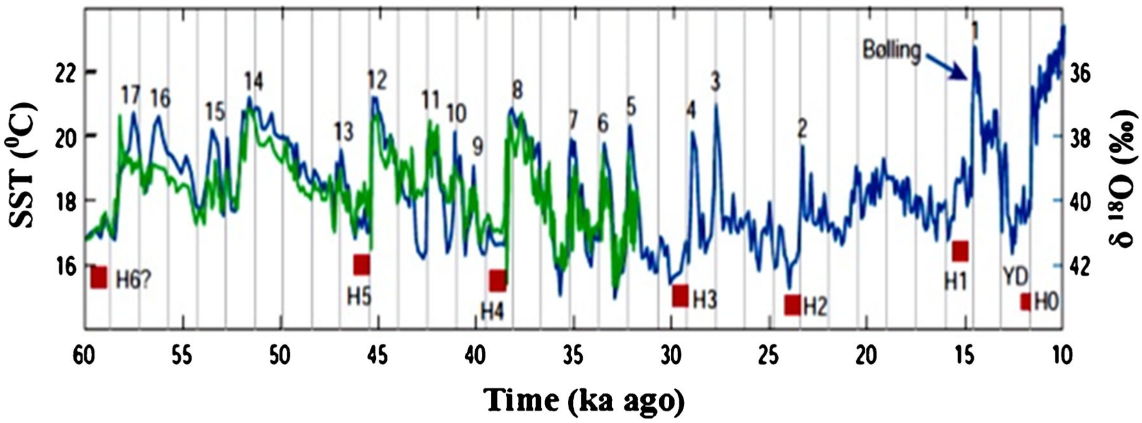

Fig. 9 Dansgaard-Oeschger (D/O) warm events (numbered) and Heinrich cold climatic events (red square) occurred during last glacial period (Rahmstorf 2002 and 2003)

glacial periods which correspond to warm climate of the D/O 2-12 events and cold climate of H2-5events.

Funding We are grateful to the Scientific and Technical Research Council of Turkey for funding this work (TÜBİTAK, project no. 114Y237).

Declarations

Conflict of interest The authors declare that they have no competing interests.

References

Algeo TJ, Maynard JB (2004) Trace-element behavior and redox facies in core shales of Upper Pennsylvanian Kansas-type cyclothems. Chem Geol 206:289–318

Blackwell BAB, Skinner AR, Blickstein JIB, Montoya AC, Florentin JA, Baboumian SM, Ahmed IJ, Deely AE (2016) ESR in the 21st century: from buried valleys and deserts to deep ocean and tectonic uplift. Earth-Sci Rev 158:125–159

Boyle J (2000) Rapid elemental analysis of sediment samples by isotope source XRF. J Paleolimnol 23:213–221

Breit GN, Wanty RB (1991) Vanadium accumulation in carbonaceous rocks: a review of geochemical controls during deposition and diagenesis. Chem Geol 91:83–97

Brennan BJ, Rink WJ, Rule EM, Schwarcz HP, Prestwich WV (1999) The ROSY ESR Dating Program. Ancient TL 17(2):45–53

Cohen AS (2003) Paleolimnology. The history and evolution of lake systems. Oxford University Press, New York

Dansgaard W, Johnsen SJ, Clausen HB, Dahl-Jensen NS, Gundestrup NS, Hammer CU, Hvidberg CS, Steffensen JP, Sveinbjörnsdottir AE, Jouzel J, Bond G (1993) Evidence for general instability of past climate from a 250-kyr ice-core record. Nature 364:218–220

de Oliveira SMB, Saia SEMG, Pessenda LCR, Favora DIT (2009) Lacustrine sediments provide geochemical evidence of environmental change during the last millennium in southeastern Brazil. Chemie Der Erde - Geochemistry 69:395–405

de Ridder NA (1965) Sediments of the Konya basin, Central Anatolia, Turkey. Paleogeography, Paleoclimatology, Paleoecology 1:225–254

Dymond J, Suess E, Lyle M (1992) Barium in deep-sea sediments: a geochemical proxy for paleoproductivity. Paleoceanography 7: 163–181

Eusterhues K, Heinrichs H, Schneider J (2005) Geochemical response on redox fluctuations in Holocene lake sediments, Lake Steisslingen, Southern Germany. Chem Geol 222:1–22

Fernex F, Février G, Benaïm J, Arnoux A (1992) Copper, lead and zinc trapping in Mediterranean deep-sea sediments: probable coprecipitation with manganese and iron. Chem Geol 98:293–308

Fontugne M, Kuzucuoğlu C, Karabıyıkoğlu M, Hatte C, Pastre CF (1999) From Pleniglacial to Holocene: a ^{14}C chronostratigraphy of environmental changes in the Konya Plain, Turkey. Quat Sci Rev 18:573–591

Francois R, Honjo S, Manganini SJ, Ravizza GE (1995) Biogenic barium fluxes to the deep sea: implications for paleoproductivity reconstruction. Glob Biogeochem Cycles 9(2):289–303

Grün R (1989) Electron Spin Resonance (ESR) Dating. Quat Int 1:65–109

Guimaraes JTF, Sahoo PK, Souza-Filho WM, Maurity CW, Junior ROS, Costa FR, Dall'agnol R (2016) Late Quaternary environmental and climate changes registered in lacustrine sediments of the Serra Sul de Carajas, south-east Amazonia. J Quat Sci 31(2):61–74

Hermanowski B, Costa ML, Carvalho AT, Behling H (2012) Paleoenvironmental dynamics and underlying climatic changes in southeast Amazonia (Serra Sul de Carajas, Brazil) during the late Pleistocene and Holocene. Paleogeography Paleoclimatology Paleoecology 365–366:227–246

Hodell DA, Anselmetti FS, Ariztegui D, Brenner M, Curtis JH, Gilli A, Grzesik DA, Guilderson TJ, Müller AD, Bush MB, Correa-Metrio A, Escobar J, Kutterolf S (2008) An 85-ka record of climate change in lowland Central America. Quat Sci Rev 27:1152–1165

Ikeya M (1993) New Applications of Electron Spin Resonance, Dating Dosimetry and Microscopy. World Scientific Pub. Co. Pte. Ltd.

Jeandel C, Tachikawa K, Bory A, Dehairs F (2000) Biogenic barium in suspended and trapped material as a tracer of export production in tropical NE Atlantic (EUMELI sites). Mar Chem 71:125–142

Johnsen SJ, Clausen HB, Dansgaard W, Fuhrer K, Gundestrup N, Hammer CU, Iversen P, Jouzel J, Stauffer B, Steffensen JP (1992) Irregular glacial interstadials recorded in a new Greenland ice core. Nature 359:311–313

Jones B, Manning DAC (1994) Comparison of geochemical indices used for the interpretation of paleoredox conditions in ancient mudstones. Chem Geol 111:111–129

Karabıyıkoğlu M, Kuzucuoğlu C, Fontugne M, Kaiser B, Mouralis D, Babayigit S (1999) Facies and depositional sequences of the Late Pleistocene Göçü shoreline system, Konya basin, Central Anatolia: implications for reconstructing lake-level changes. Quat Sci Rev 18: 593–609

Kidder DL, Erwin DH (2001) Secular distribution of biogenic silica through the Phanerozoic: comparison of silica-replaced fossils and bedded cherts at the series level. J Geol 109:509–522

Kochenov AV, Korolev KG, Dubinchuk VT, Medvedev YL (1977) Experimental data on the conditions of precipitation of uranium from aqueous solutions. Geochem Int 14:82–87

Koinig KA, Shotyk W, Lotter AF, Ohlendorf C, Strum M (2003) 9000 years of geochemical evolution of lithogenic major and trace elements in the sediment of an alpine lake-the role of climate, vegetation, and land-use history. J Paleolimnol 30:307–320

Kuzucuoğlu C, Karabıyıkoğlu M, Parish R (1998) The dune systems of the Konya Plain (Turkey) Their relation to the environmental changes in Central Anatolia during Late Pleistocene and Holocene. Geomorphology 23:257–271

Lei C, Hongyuan S, Yulian J, Jinglu W, Xusheng L, Ling W, Pengling W (2008) Environmental change inferred from Rb and Sr of lacustrine sediments in Huangqihai Lake, Inner Mongolia. J Geogr Sci 18: 373–384

Lewan MD, Maynard JB (1982) Factors controlling the enrichment of vanadium and nickel in the bitumen of organic sedimentary rocks. Geochim Cosmochim Acta 46:2547–2560

Lowe JJ, Walker MJC (1997) Reconstructing quaternary environments. Longmans, London, (Third edition)

Martín-Puertas C, Valero-Garcés BL, Mata MP, Moreno A, Giralt S, Martinez-Ruiz F, Jiménez-Espejo F (2011) Geochemical processes in a Mediterranean Lake: a high-resolution study of the last 4, 000 years in Zoñar Lake, southern Spain. J Paleolimnol 46:405–421

Mayr C, Fey M, Haberzettl T, Janssen S, Lücke A, Maidana NI, Ohlendorf C, Schäbitz F, Schleser GH, Struck U, Wille M, Zolitschka B (2005) Paleoenvironmental changes in southern Patagonia during the last millennium recorded in lake sediments from Laguna Azul (Argentina). Paleogeography Paleoclimatology Paleoecology 228:203–227

Monnin C, Jeandel C, Cattaldo T, Dehairs F (1999) The marine barite saturation state of the world's oceans. Mar Chem 65:253–261

Moreno A, Valero-Garcés BL, González-Sampériz P, Rico M (2008) Flood response to rainfall variability during the last 2000 years inferred from the Taravilla lake record (Central Iberian Range, Spain). J Paleolimnol 40:943–961

Murphy AE, Sageman BB, Hollander DJ, Lyons TL, Brett C (2000) Black shale deposition and faunal overturn in the Devonian Appalachian Basin: clastic starvation, seasonal water-column mixing, and efficient biolimiting nutrient recycling. Paleoceanography 15:280–291

Orhan H, Delikan A, Demir A, Kapan S, Olgun K, Özmen A, Sayın Ü, Ekici G, Aydın H, Nazik A (2019) Geochemical evidences of paleoenvironmental changes in Late Quaternary lacustrine sediments of the Konya Closed Basin Konya, Turkey. In: Zhang Z et al (eds) Patterns and Mechanisms of Climate, Paleoclimate and Paleoenvironmental Changes from Low-Latitude Regions. Advances in Science, Technology & Innovation, pp 73–76

Piper DZ, Perkins RB (2004) A modern vs. Permian black shale—the hydrography, primary productivity, and water-column chemistry of deposition. Chem Geol 206:177–197

Rahmstorf S (2002) Ocean circulation and climate during the past 120, 000 years. Nature 419:207–214

Rahmstorf S (2003) Timing of abrupt climate change: a precise clock. Geophysical Research Letters Nature 30(10):17.1–17.4

Roberts N (1983) Age, paleoenvironments, and climatic significance of Late Pleistocene Konya Lake, Turkey. Quat Res 19:154–171

Roberts N, Erol O, de Meester T, Uerpmann HP (1979) Radiocarbon chronology of Late Pleistocene Konya lake, Turkey. Nature 281: 662–664

Roberts N, Black S, Boyer P, Eastwood WJ, Griffiths H, Lamb HF, Leng M, Parish R, Reed J, Twigg D, Yiğitbaşoğlu H (1999) Chronology and stratigraphy of Late Quaternary sediments in the Konya Basin, Turkey: Results from the KOPAL project. Quat Sci Rev 18:611–630

Sahoo PK, Souza-Filho PWM, Guimaraes JTF, da Silva MS, Costa FR, Manes C-LO, Oti D, Silva Júnior RO, Dall'Agnol R (2015) Use of multi-proxy approaches to determine the origin and depositional processes in modern lacustrine sediments: Caracas Plateau, Southeastern Amazon, Brazil. Appl Geochem 52:130–146

Schnetger B, Brumsack H-J, Schale H et al (2000) Geochemical characteristics of deep-sea sediments from the Arabian Sea: a high-resolution study. Deep-Sea Res II Top Stud Oceanogr 47:2735–2768

Selig U, Leipe T, Dörfler W (2007) Paleolimnological record of nutrient and metal profile in prehistoric, historic and modern sediments of three lakes in north-eastern Germany. Water Air Soil Pollut 184: 183–194

Tanaka K, Akagawa F, Yamamote K, Tani Y, Kawabe I, Kawai T (2007) Rare earth elements geochemistry of Lake Baikal sediment: its implication for geochemical response to climate change during the Last Glacial/Interglacial transition. Quat Sci Rev 26:1362–1368

Tribovillard N, Algeo TJ, Lyons T, Riboulleau A (2006) Trace metals as paleoredox and paleoproductivity proxies: an update. Chem Geol 232:12–32

Wignall PB, Twitchett RJ (1996) Oceanic anoxia and the end Permian mass extinction. Science 272:1155–1158

Zhao J, Jin Z, Jin Z, Geng Y, Wen X, Yan CB (2016) Applying sedimentary geochemical proxies for paleoenvironment interpretation of organic-rich shale deposition in the Sichuan Basin, China. Int J Coal Geol 163:52–71